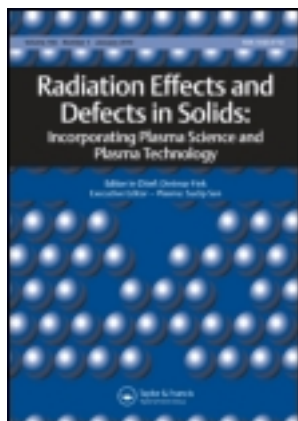


This article was downloaded by: [UNAM Ciudad Universitaria]

On: 11 October 2011, At: 09:53

Publisher: Taylor & Francis

Informa Ltd Registered in England and Wales Registered Number: 1072954 Registered office: Mortimer House, 37-41 Mortimer Street, London W1T 3JH, UK



Radiation Effects and Defects in Solids

Publication details, including instructions for authors and subscription information:

<http://www.tandfonline.com/loi/grad20>

Optimization and thermal stability studies of Ignitor and ITER

Julio J. Martinell^a

^a Instituto de Ciencias Nucleares, Universidad Nacional Autónoma de México, A. Postal 70-543, Mexico D.F., Mexico

Available online: 07 Oct 2011

To cite this article: Julio J. Martinell (2011): Optimization and thermal stability studies of Ignitor and ITER, Radiation Effects and Defects in Solids, 166:10, 821-828

To link to this article: <http://dx.doi.org/10.1080/10420150.2011.617751>

PLEASE SCROLL DOWN FOR ARTICLE

Full terms and conditions of use: <http://www.tandfonline.com/page/terms-and-conditions>

This article may be used for research, teaching, and private study purposes. Any substantial or systematic reproduction, redistribution, reselling, loan, sub-licensing, systematic supply, or distribution in any form to anyone is expressly forbidden.

The publisher does not give any warranty express or implied or make any representation that the contents will be complete or accurate or up to date. The accuracy of any instructions, formulae, and drug doses should be independently verified with primary sources. The publisher shall not be liable for any loss, actions, claims, proceedings, demand, or costs or damages whatsoever or howsoever caused arising directly or indirectly in connection with or arising out of the use of this material.

Optimization and thermal stability studies of Ignitor and ITER

Julio J. Martinell*

*Instituto de Ciencias Nucleares, Universidad Nacional Autónoma de México, A. Postal 70-543,
Mexico D.F., Mexico*

(Received 21 May 2011; final version received 22 August 2011)

A comparison between the operational states of Ignitor and ITER needed to obtain a maximal energy gain is presented for a range of temperatures and densities, under the assumption that the ratio of electron to ion temperatures is held fixed for all the steady states considered. A criterion for the optimal operation of ITER is obtained in terms of the auxiliary heating to ions. The optimal states for Ignitor are achieved when auxiliary heating to both ions and electrons is minimized. The thermal stability is also studied for the same range of parameters, finding that the development of this instability is not a concern for ITER, while a certain range of plasma densities and temperatures has to be maintained in order to avoid the thermonuclear instability in Ignitor.

Keywords: fusion reactors; burning plasmas; thermal stability; optimal operation

PACS: 28.52.-s; 52.25.Xz; 52.35.Py; 52.55.Dy

1. Introduction

The next generation of fusion experiments will be focused on creating and studying burning plasmas where heating from fusion reactions will be a dominant part or even the only one when ignition is achieved. The behavior of plasmas in this state will have to be thoroughly explored in order to check if the theoretical predictions are correct. Most efforts in that direction are being directed toward ITER, which is currently under construction in France, although it is designed to just reach an energy gain value of $Q = 10$. Another proposed experiment is Ignitor, whose construction is still being planned under an agreement between Italy and Russia. This apparatus will have the potential to reach ignition, allowing the study of a wider range of plasmas in a shorter term. In any of these machines, in order to optimize the performance, it is necessary to minimize the auxiliary heating requirements, which will ideally be zero for an ignited plasma. The optimal operation should maximize the energy gain factor Q for a given fusion energy production and this operation point would be maintained by a control system. A possible control system may be based on an artificial neural network that manages the fuel injection rate and the auxiliary power (I). In this work, we analyze the burn regimes of ITER and Ignitor for different plasma parameters, using a zero-dimensional, two-temperature model in which energy and particle transports are

*Email: martinell@nucleares.unam.mx

accounted for by global confinement times for energy τ_E , fuel particles τ_{DT} and alpha particles τ_α . The operating points studied in this work are constrained to keep the ratio T_e/T_i constant, and the global transport of ions and electrons is assumed to be the same.

Another important issue in the operation of burning plasmas is the stability of the optimal states under the thermonuclear instability, which arises when the fusion power produces a positive feedback in the plasma temperature. At a certain temperature range, the fusion reaction rate is an increasing function of temperature, which produces more fusion power as the temperature rises, leading to an instability if the power losses are not large enough. We study the stability of the operational states around the optimal points in order to make sure that the thermonuclear instability is not a threat to a safe operation. Our analyses are based on Plasma OPERATION CONtours (POPCON) plots in the electron density n_e and temperature T_e space, where the appropriate range of parameters can be identified.

2. Model equations

The model is based on the equations for particle conservation for the main ions, which are assumed to be composed of a 50–50 mixture of deuterium and tritium, and for the alpha particles resulting from the fusion reactions, together with energy conservation for ions and electrons. The multi-fluid description for the plasma produces four equations for the total deuterium–tritium (D–T) density n_{DT} , alpha particle density n_α and the electron and ion temperatures T_e and T_i . The quasineutrality condition $n_e = n_{DT} + 2n_\alpha + Z_{Be}n_{Be} + Z_{Ar}n_{Ar}$ is assumed and two impurity species (Be and Ar) are included, but we assume that they are fixed. The equations are as follows:

$$\frac{\partial}{\partial t} n_{DT} = S_f - \frac{1}{2} n_{DT}^2 \langle \sigma v \rangle - \nabla \cdot \vec{\Gamma}_{DT}, \quad (1)$$

$$\frac{\partial}{\partial t} n_\alpha = \frac{1}{4} (1 - f_{frac}) n_{DT}^2 \langle \sigma v \rangle - \nabla \cdot \vec{\Gamma}_\alpha, \quad (2)$$

$$\begin{aligned} \frac{\partial}{\partial t} \left[\frac{3}{2} n_e T_e \right] = & \mathcal{P}_{aux,e} + \frac{1}{4} (1 - f_{frac}) f_e Q_\alpha n_{DT}^2 \langle \sigma v \rangle + \mathcal{P}_{OH} - \mathcal{P}_{brem} \\ & - \mathcal{P}_{cycl} - \frac{3 n_e (T_e - T_i)}{2 \tau_{ei}} - \nabla \cdot \vec{\Gamma}_{E,e} \end{aligned} \quad (3)$$

$$\begin{aligned} \frac{\partial}{\partial t} \left[\frac{3}{2} (n_{DT} + n_\alpha + n_{Be} + n_{Ar}) T_i \right] = & \mathcal{P}_{aux,i} + \frac{1}{4} (1 - f_{frac}) f_i Q_\alpha n_{DT}^2 \langle \sigma v \rangle \\ & + \frac{3 n_e (T_e - T_i)}{2 \tau_{ei}} - \nabla \cdot \vec{\Gamma}_{E,i}, \end{aligned} \quad (4)$$

where the electron energy losses and sources include bremsstrahlung \mathcal{P}_{brem} and cyclotron radiation \mathcal{P}_{cycl} , ohmic heating \mathcal{P}_{OH} , fusion power (in terms of the D–T reactivity $\langle \sigma v \rangle$) and auxiliary power $\mathcal{P}_{aux,e}$. For ions, there is only fusion and auxiliary power $\mathcal{P}_{aux,i}$. There is also the electron–ion energy exchange measured by the relaxation time τ_{ei} . The expression that we use for the reactivity is from (2). Thermalization of the alpha particles produced by fusion is assumed to be instantaneous. The birth energy of the alpha particles is $Q_\alpha = 3.5$ MeV; f_{frac} is the effective fraction of alpha particles which are anomalously lost due to magnetohydrodynamic (MHD) events before they are thermalized; and f_e and f_i are the fractions of the alpha particle energy Q_α deposited to the electrons and to the ions, respectively.

The fluxes Γ_k are not considered explicitly because of the poor understanding of particle and energy plasma transport, and instead we take a volume average of the fluid equations, which reduces the transport losses to the use of confinement times for the electron and ion energies $\tau_{E,e}$ and $\tau_{E,i}$, as well as for the particle number of D–T and helium ash τ_p and τ_α , respectively. This

operation simplifies the model to zero dimensions, since all the radial variation of the plasma quantities is washed out. We do this in two different ways:

(a) Assume constant density profiles $n_k(r) = n_{k0}$ and radial temperature profiles for both ions and electrons of the form

$$T_k(r, t) = T_{k0}(t) \left[1 - \left(\frac{r}{a} \right)^2 \right]^\gamma, \quad (5)$$

with T_{k0} being the central temperature of each species and a being the tokamak minor radius. This was adopted for the ITER analyses. The flat $n(r)$ is justified for the H mode in the confinement region, which is the mode considered for ITER.

(b) Obtain the $n_k(r)$ and $T_k(r)$ profiles from transport simulations using the Astra transport code (3), corresponding to a steady-state operation with a reference state. Since a certain radial transport information is conveyed in this way, we can call this a half-dimensional model. This was followed for the Ignitor studies.

The volume-averaged equations for steady-state operation, which are expressed in terms of the central temperatures and density (the 0 subscript is dropped for shortness), take the form

$$S_f - \frac{1}{2} n_{\text{DT}}^2 \langle \sigma v \rangle_{\text{vol}} - \frac{n_{\text{DT}}}{\tau_p} = 0, \quad (6)$$

$$\frac{1}{4} (1 - f_{\text{frac}}) n_{\text{DT}}^2 \langle \sigma v \rangle_{\text{vol}} - \frac{n_\alpha}{\tau_\alpha} = 0, \quad (7)$$

$$\begin{aligned} \mathcal{P}_{\text{aux,e}} + \frac{Q_\alpha}{4} (1 - f_{\text{frac}}) f_e n_{\text{DT}}^2 \langle \sigma v \rangle_{\text{vol}} - \frac{3}{2} f_{\text{pe}} \frac{n_e T_e}{\tau_E} - \frac{3}{2} f_{\text{ex}} n_e \frac{T_e - T_i}{\tau_{ei}} \\ + A_h \frac{Z_{\text{eff}}^{1/2}}{T_e^{3/2}} \left(\frac{1 + 1.198 Z_{\text{eff}}^{1/2} + 0.22 Z_{\text{eff}}}{1 + 2.97 Z_{\text{eff}}^{1/2} + 0.75 Z_{\text{eff}}} \right) f_{\text{OH}} - A_b Z_{\text{eff}} f_{\text{rad}} n_e^2 T_e^{1/2} \\ - A_{\text{cyc}} f_R n_e^{1/2} T_e^{2.5} \frac{1 + 1.93 T_e / 511}{1 - 0.58 T_e / 511} \left(1 + \frac{18a}{R \sqrt{T_e}} \right)^{1/2} = 0, \end{aligned} \quad (8)$$

$$\mathcal{P}_{\text{aux,i}} + \frac{Q_\alpha}{4} (1 - f_{\text{frac}}) f_i n_{\text{DT}}^2 \langle \sigma v \rangle_{\text{vol}} + \frac{3}{2} f_{\text{ex}} n_e \frac{T_e - T_i}{\tau_{ei}} - \frac{3}{2} f_{\text{pe}} n_i \frac{T_i}{\tau_E} = 0, \quad (9)$$

where $n_i = n_{\text{DT}} + n_\alpha + n_{\text{Be}} + n_{\text{Ar}}$ and the averaged power densities are given explicitly in MW/m^3 , with $A_b = 5.33 \times 10^{-43}$, $A_h = 0.032$, $A_{\text{cyc}} = 2.9 \times 10^{-17} k^{5/6} / (B^5 a)^{0.5}$ for n , and T in m^{-3} , keV. The f factors include the profile averaging weight and, as such, depend on the shape of the profiles. The volume-averaged D–T reactivity can be written as $\langle \sigma v \rangle_{\text{vol}} = G \times \langle \sigma v \rangle$, where G is a correction factor due to the radial profile average.

For our analysis, we use the energy gain factor Q_G defined as the ratio of the energy generation rate in the plasma due to the fusion reactions to the total external heating power:

$$Q_G = \frac{\langle \mathcal{P}_{\text{fusion}} \rangle_{\text{vol}}}{\langle \mathcal{P}_{\text{aux}} + \mathcal{P}_{\text{ohmic}} \rangle_{\text{vol}}}. \quad (10)$$

Here, \mathcal{P}_{aux} includes both the auxiliary heating to electrons and to ions and $\mathcal{P}_{\text{fusion}}$ takes into account the total energy produced in the D–T fusion reactions, that is, the energy carried by the alpha particles and by the neutrons. If operation in the H mode is desired, total power has to be maintained above the L–H power threshold (4),

$$P_{\text{threshold}} = 4.30 M_{\text{eff}}^{-1} B^{0.772} n_e^{0.782} R^{0.999} a^{0.975}. \quad (11)$$

In the following analysis, we solve Equations (6)–(9) for the DT refueling rate, S_f , the fractional density of helium ash, f_α , and the auxiliary heating power to electrons and ions, $\mathcal{P}_{\text{aux,e}}$ and $\mathcal{P}_{\text{aux,i}}$, varying n_e and T_e over a range about the reference state.

3. Optimal operating states for ITER and Ignitor

3.1. ITER

The operational states for ITER have been presented in (5) for a fixed *fraction* of Be impurities of $f_{\text{Be}} = 0.02$ and a fixed *density* of Ar of $n_{\text{Ar}} = 1.21 \times 10^{17} \text{ m}^{-3}$. The fudge factors corresponding to Equation (5) and with the weights needed to match the design values for ITER are as follows: $f_{\text{OH}} = 7.5(1 + \frac{3}{2}\gamma)$, $f_{\text{pe}} = 1/(1 + \gamma)$, $f_{\text{ex}} = (1 + 3\gamma/2)/(1 + \gamma)$, $f_{\text{R}} = (1 + \frac{5}{2}\gamma)^{-1}$ and $f_{\text{rad}} = 2/(1 + \gamma/2)$, the factor 2 meant to account for the combined bremsstrahlung and line radiated power reported at the nominal density and temperatures for ITER (6), which compensates for the lack of a line radiation term in the energy balance equations. The G factor of $\langle\sigma v\rangle$ is fitted by a polynomial

$$G = 0.249 + 0.017T_i - 0.00011T_i^2 - 0.13\gamma + 0.023\gamma^2 - 0.0077\gamma T_i + 0.00125T_i\gamma^2 + 0.000067T_i^2\gamma - 0.0000126T_i^2\gamma^2, \quad (12)$$

where T_i is the central ion temperature in keV and $\langle\sigma v\rangle$ is the reactivity evaluated at the central ion temperature. The value of τ_E is taken from the IPB98(y,2) scaling (7):

$$\tau_{\text{IPB98}(y,2)} = 0.0562HI^{0.93}R^{1.97}B^{0.15}M^{0.19}\epsilon^{0.58}k^{0.78}n_e^{0.41}P_s^{-0.69}, \quad (13)$$

where the factor H expresses the degree of enhancement expected over the predicted value due to improved confinement, but we set $H = 1$.

The calculated values for the fraction of energy deposited to electrons and to ions in the energy range of the alpha particle thermalization are $f_e = 0.78$ and $f_i = 0.22$. The reference operating state has $n_0 = 1.01 \times 10^{20} \text{ m}^{-3}$, $T_{e0} = 23.6 \text{ keV}$ and $T_{i0} = 23.0 \text{ keV}$, for the electron density and the peak temperatures of the electrons and the ions, respectively. The radial profile parameter is $\gamma = 1.85$ for both electron and ion temperatures. It is assumed that 10% of the alpha particles are anomalously lost before they are thermalized, hence $f_{\text{frac}} = 0.1$ and the confinement times are $\tau_\alpha = 6.8\tau_E$ and $\tau_{\text{DT}} = \tau_\alpha$ for DT ions. The corresponding value of the fixed temperature ratio is $(T_e - T_i)/T_e = 0.025$ for all the operation states considered.

Possible steady states can be classified according to the values of different parameters of interest. Important information about the operation states can be gained from Figure 1(a), which shows the contour plots of the auxiliary heating power to electrons and ions in POPCON plots (normalized $T_e - n_e$ space) with isolines for these quantities. It can be seen that for a constant electron density, the auxiliary heating power to the ions decreases when T_e decreases reaching a point where $P_{\text{aux},i} = 0$. Note that the contour lines with $P_{\text{aux},i} < 0$ are not included because these are not physically plausible steady states. Thus, the line $P_{\text{aux},i} = 0$ represents a boundary for the available operating points of the reactor.

Figure 1(b) shows the contour lines of the gain factor, Q_G , as obtained from Equation (10) and for constant total fusion power (including the energy of the neutrons), together with the boundary line $P_{\text{aux},i} = 0$. We can observe that for a fixed fusion power value, we can decrease the electron temperature increasing simultaneously the electron density, properly moving along the corresponding $P_{\text{fusion}} = \text{constant}$ line, thus increasing the Q_G monotonically until the boundary $P_{\text{aux},i} = 0$ is reached. Thus, the optimal states, defined as those having a maximum Q_G for a given P_{fusion} , correspond to the crossings with boundary line $P_{\text{aux},i} = 0$. Note that the H-mode operation has to be to the right of the magenta line (color online) which represents the L–H transition power threshold.

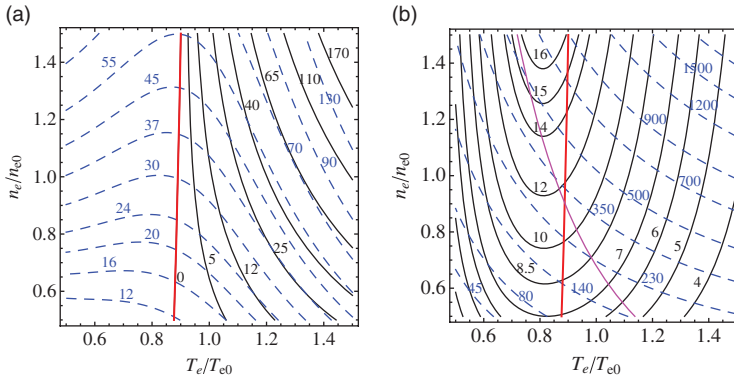


Figure 1. Contour curves of (a) auxiliary power to electrons, $P_{aux,e}$ (dashed line), and to ions, $P_{aux,i}$ (solid line) and (b) total fusion power in MW (dashed line) and the Q -gain factor. Lines of $P_{aux,i} = 0$ (red, from (a)) and L-H transition threshold (magenta) are shown (color online).

3.2. Ignitor

Ignitor is proposed to be the first nuclear fusion experiment ever to achieve ignition. It has been extensively studied under several operation scenarios, in particular, its operation in an ignited state with only ohmic heating (8). Auxiliary heating will be present in the form of ion cyclotron resonance heating (ICRH) in order to aid in reaching the high temperatures required, but in ignition, ICRH will be shut down. We analyze the possible operational states around the design reference state given in Table 1 for operation in the L mode.

For this study, we will use the half-dimensional approach mentioned above, obtaining the profiles from Astra transport simulations. To do this, an initial state is provided and the code evolves until a steady state is reached with the design values of the Ignitor plasma. In order to get to this state, some weight factors are varied during the run. Once this is achieved, the resulting profiles are used to determine the volume average of the conservation equations. Thus, the corresponding fudge factors are obtained, and for the reference state, we have the following values: $f_{OH} = 200$, $f_{pe} = 0.2$, $f_{ex} = 0.34$, $f_R = 0.1$ and $f_{rad} = 0.21$, while $G = 0.056$. For the confinement time τ_E , the Coppi–Mazzucato–Gruber (CMG) scaling is used,

$$\tau_{CMG} = HI^{-1} a^3 T_e \left(\frac{M}{Z_{eff}} \right)^{-0.4} (1 + \kappa^2) \kappa^{-0.5} n_e^{0.8}, \quad (14)$$

where again $H = 1$. The values for Ignitor for the fraction of energy deposited to electrons and to ions are $f_e = 0.81$ and $f_i = 0.19$. The reference operating state has $n_0 = 9.97 \times 10^{20} \text{ m}^{-3}$, $T_{e0} = 10.7 \text{ keV}$ and $T_{i0} = 10.4 \text{ keV}$, $f_{frac} = 0$ and the confinement times are $\tau_\alpha = 6\tau_E$ and $\tau_{DT} = 3\tau_\alpha$ for DT ions. The fixed temperature ratio is $(T_e - T_i)/T_e = 0.028$. The density is below the Greenwald limit $n_G/n_0 = 1.59$.

Table 1. Ignitor parameters.

| | | | | | |
|------------------------|--------------|-----------------------------|----------------------|------------------------------|----------------------|
| Major radius | R_0 | 1.32 m | Mean poloidal field | $\bar{B}_p = I_p/5\sqrt{ab}$ | $\leq 4.5 \text{ T}$ |
| Minor radius | $a \times b$ | $.47 \times 0.86 \text{ m}$ | Poloidal current | I_θ | $\leq 9 \text{ MA}$ |
| Aspect ratio | A | 2.8 | Edge safety factor | q_ψ | 3.6 |
| Elongation | κ | 1.83 m | Confinement strength | $S_c \equiv I_p \bar{B}_p$ | 38 MA-T |
| Triangularity | δ | 0.4 | Plasma volume | V | 10 m^3 |
| Toroidal field | B_T | $\leq 13 \text{ T}$ | Plasma surface | S | 34 m^2 |
| Toroidal current | I_p | 11 MA | ICRH heating | 100–140 MHz | $\leq 20 \text{ MW}$ |
| Maximum poloidal field | $B_{p,max}$ | $\leq 6.5 \text{ T}$ | Optimal ICRH heating | 115 MHz | 3–5 MW |

In Figure 2(a), the contour plots of $P_{\text{aux},e}$ and $P_{\text{aux},i}$ are shown for only the positive values. It is clear that a significant region of the $n - T_e$ space is not accessible in the considered operation conditions; only the parameter ranges where both $P_{\text{aux},e}$ and $P_{\text{aux},i}$ are positive are possible. These are islands of operation. Examining Figure 2(b), which shows the contours of constant Q_G and P_{fusion} , it is possible to note that the high-density island is the one that has the highest fusion powers and Q_G values; a state with $Q_G = 8$ can be achieved in the high-temperature side. This is thus the preferred region of operation. In contrast with the ITER situation, here a fixed fusion power provides higher Q_G values when the density is decreased and the temperature is increased, but the differences are not very important since the two isolines are quite similar. The optimization criterion would be to operate at the high-temperature side of the upper island, where $P_{\text{aux},e} = P_{\text{aux},i} = 0$. At this point, one will have an ignited plasma, not requiring external power.

4. Thermal stability

The optimal steady states just obtained have to be checked for stability under thermal fluctuations. Temperature scalings of all the terms in the energy equations compete to determine stability. In particular, radiation losses, which take an important fraction of the fusion energy, are of prime importance and they also, like the fusion power for low T , have a growing dependence with temperature (both bremsstrahlung and cyclotron radiation). The thermonuclear instability arises when the temperature rise due to the energy released by the fusion reactions increases the DT reactivity further, and this occurs in the energy range with a positive slope of the function $\langle\sigma v\rangle(T)$, that is, $T < 50$ keV. In order to study this instability, we apply a thermal perturbation to the system and analyze its response. We consider two different cases: (a) equal temperatures, $T_i = T_e \equiv T$, and (b) two temperatures, $T_i \neq T_e$, as in the analysis of the optimal states. The first case is taken as a simple approximation, for in this case, there is a single equation for the total energy $W = W_e + W_i$. Performing a linear analysis, when a perturbation of the form $T = T_0 + \delta T$ on the equilibrium value T_0 is applied, the total energy equation can be expanded in δT and takes the form

$$\frac{\partial \delta T}{\partial t} = \left[\frac{dP(T_0)}{dT} \right] \delta T, \quad (15)$$

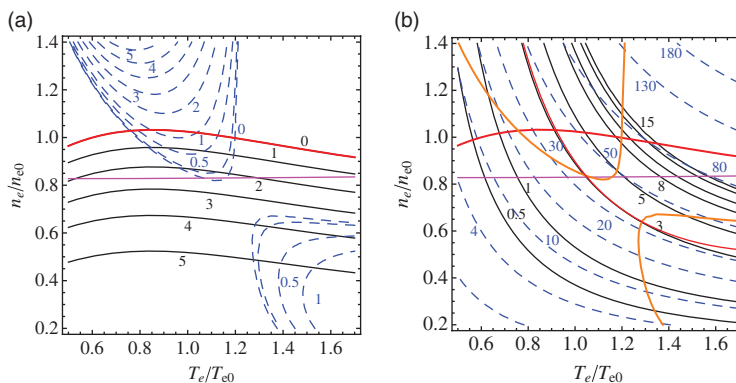


Figure 2. Isolines for Ignitor of constant (a) auxiliary power to electrons, $P_{\text{aux},e}$ (dashed line), and to ions, $P_{\text{aux},i}$ labeled in MW (only positive values are plotted) and (b) total fusion power in MW (dashed line) and the Q_G -gain factor. Red and orange lines indicate limits $P_{\text{aux},e} = 0$ and $P_{\text{aux},i} = 0$ from (a). Below the magenta line H-mode operation would occur, but these states are not considered here (color online).

where $P(T)$ is the net power to the plasma. Clearly, the perturbation is stable when the term on the right side is negative since otherwise the temperature perturbation will increase exponentially. Thus, the stability criterion is $dP(T_0)/dT < 0$. For the second case, since there are two temperatures, we have to take separate perturbations $T_e = T_{e0} + \delta T_e$ and $T_i = T_{i0} + \delta T_i$ and consider the electron and ion energy equations (3) and (4). Linearizing again about the two equilibrium temperatures, we can find an equation for the vector $\delta \mathbf{T} \equiv (\delta T_e, \delta T_i)$, as $\partial \delta \mathbf{T} / \partial t = \mathbf{M} \cdot \delta \mathbf{T}$, with the matrix

$$\mathbf{M} = \begin{pmatrix} \frac{\partial P_e(T_{0e}, T_{0i})}{\partial T_e} & \frac{\partial P_e(T_{0e}, T_{0i})}{\partial T_i} \\ \frac{\partial P_i(T_{0e}, T_{0i})}{\partial T_e} & \frac{\partial P_i(T_{0e}, T_{0i})}{\partial T_i} \end{pmatrix}, \quad (16)$$

where the powers $P_e(T_e, T_i)$ and $P_i(T_e, T_i)$ are the right-hand sides of Equations (3) and (4), respectively. The solution is obtained in terms of the eigenvalues of \mathbf{M} , λ_1 and λ_2 , as $\delta \mathbf{T} = \delta \mathbf{T}_0 \exp(\lambda_k t)$. The system will be unstable if the real part of at least one of the λ_k is positive. The stability computations are made for all the operating states in the range considered before. The marginal stability curves for ITER are presented in a POPCON plot in Figure 3(a) for the cases (a) and (b). It can be seen that the unstable region is for low T_e and high n_e , as has been found in other studies (9), for the two cases and there is actually not much difference between them. However, the region of instability falls outside the allowed operating regime since it is to the left of the green line $P_{aux,i} = 0$ (color online), thus it would not be excited for the optimal states described in Section 3 or any other allowed state.

In order to have an idea about the sensitivity of the results to the particular energy confinement scaling used, we considered a case with constant τ_E . In this analysis, τ_E is kept fixed at its equilibrium value when the variations in Equations (15) and (16) are made, instead of using Equation (13). The results are shown in Figure 3 with dashed lines for the two cases of equal and different temperatures. It is clear that the difference is quite noticeable, and now the unstable region covers all the ranges of optimal operating states. Since the constant τ_E is not compatible with the previous calculations, we cannot conclude that the instability will be present, but it shows that the choice of the actual confinement scaling is important.

In the case of Ignitor, the situation is quite different as can be seen in Figure 3(b). The marginal stability curve for the case of the CMG scaling falls right between the operational islands, which means that a large fraction of the possible operation states are unstable. In particular, the optimal states found previously for the high-temperature region are unstable. However, this confinement scaling is quite pessimistic, and if a more optimistic τ_E is used, the optimal states could become

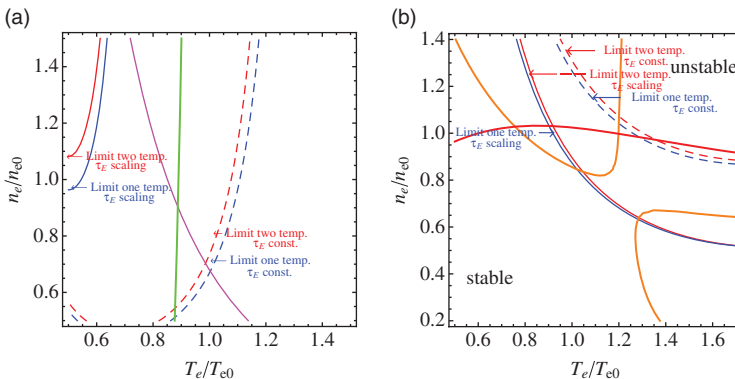


Figure 3. Marginal stability curves for (a) ITER and (b) Ignitor, with $T_e = T_i$ (blue) and $T_e \neq T_i$ (red). Dashed curves correspond to constant confinement time. The curves delimiting the allowed operation states are also shown (color online).

stable. That this is the case can be seen in the marginal stability curves shown with dashed lines which correspond to a constant τ_E , providing another extreme case; here all the allowed states are stable. Depending upon the particular scaling used, the stability curves will fall between these two curves. Practically, the same result is obtained for the two cases of equal and different electron/ion temperatures. If one could use a certain scaling that is reliable and it turns out there is a region of unstable states, then a control system for the machine has to be used in order to avoid these states.

5. Conclusions

We have studied the plasmas of two burning plasma fusion experiments, ITER and Ignitor, in order to determine the most efficient operation of a nuclear fusion reactor, by means of volume-averaged balance equations for particles and energy, including electrons, ions and helium ash. Nominal operation states were taken for each experiment and the steady states of operation about these states were analyzed by taking variations of the electron density and temperature, maintaining the temperature ratio T_e/T_i fixed. They are presented in POPCON plots showing contours of constant auxiliary power to electrons and ions. In the case of ITER, no states with $P_{\text{aux}} = P_{\text{aux},e} + P_{\text{aux},i} = 0$ can occur, meaning that ignition is not possible, as expected. However, there are states with $P_{\text{aux},i} = 0$, which represent an operational boundary and they turn out to be also the states with maximum Q_G for a given fusion power. Hence, we identified these operational states as the optimal ones.

In the case of Ignitor, the range of operational states is more restricted and it is possible to identify those with largest energy gain as those in the high-density, high-temperature region. Among these states, there is the ignition state for which the total external power is zero.

The thermonuclear stability was studied using linear analysis by considering temperature perturbations about the equilibrium state. Cases with $T_e = T_i$ and $T_e \neq T_i$ were considered. For ITER, we showed that the system will be stable for all the possible operating states regardless of the relation $T_e - T_i$. The assumed scaling for τ_E is important and a constant scaling may render some states unstable in the high-density–low-temperature range, including the optimal states. In the case of Ignitor, the pessimistic CMG scaling produces unstable states in the region of optimal operation, but for more optimistic scaling, these become stable.

Acknowledgements

This work was partially supported by DGAPA-UNAM project IN106911-3.

References

- (1) Vitela, J.E.; Martinell, J.J. *Plasma Phys. Control. Fusion* **2001**, *43*, 99–119.
- (2) Bosch, H.S.; Hale, G.M. *Nucl. Fusion* **1992**, *32*, 611–632.
- (3) Pereverzev, G.; Yushmanov, P. *ASTRA: Automated System of TRansport Analysis*; IPP Report 5/98; Max-Planck-Institut für Plasmaphysik: Garching, 2002.
- (4) Martin, Y.R.; Takizuka, T. *J. Phys. Conf. Ser.* **2008**, *123*, 012033.
- (5) Martinell, J.J.; Vitela, J.E. *J. Phys. Conf. Ser.* **2011**, forthcoming.
- (6) ITER Physics Basis. *Nucl. Fusion* **1999**, *39*, No. 12.
- (7) Aymar, R.; Barabaschi, P.; Shimomura, Y. *Plasma Phys. Control. Fusion* **2002**, *44*, 519–566.
- (8) Coppi, B.; Airoidi, A.; Bombarda, F.; Cenacchi, G.; Detragiache, P.; Sugiyama, L.E. *Nucl. Fusion* **2001**, *41*, 1253–1257.
- (9) Mandrekas, J.; Stacey, W.M. *Fusion Technol.* **1991**, *19*, 57–77.